Energy Conversion and Management 348 (2026) 120791

Contents lists available at ScienceDirect

Energy Conversion and Management

journal homepage: www.elsevier.com/locate/enconman

Research Paper

Techno-economic optimization of agrivoltaic-powered anaerobic digestion plant for biomethane production

Amirhossein Nik Zad [a,*], Sebastian Zainali [b], Michele Croci [a], Mohammed Guezgouz [b], Giorgio Impollonia [a], Pietro Elia Campana [b], Stefano Amaducci [a]

[a] Department of Sustainable Crop Production, Università Cattolica del Sacro Cuore, Piacenza, Italy
[b] Department of Sustainable Energy Systems, Mälardalen University, Västerås, Sweden

ARTICLE INFO

Keywords:
Agrivoltaic
Photovoltaic
Optimization
Anaerobic digestion
Biogas
Biomethane
TOPSIS

ABSTRACT

Decarbonizing biomethane facilities demands integrated electricity-heat strategies respecting land constraints. This study presents the first optimization framework integrating bifacial agrivoltaic systems with anaerobic digestion plants for biomethane production, addressing a critical gap in renewable energy system design. A multi-objective genetic algorithm coupled with Technique for Order Preference by Similarity to Ideal Solution ranking methodology was developed to simultaneously optimize economic performance and land utilization across three distinct agrivoltaic configurations including fixed vertical, 1-axis, and 2-axis tracking systems. The framework evaluates eight scenarios encompassing on-grid agrivoltaic systems with various heating technologies (biogas boilers, groundwater heat pumps, and biogas combined heat and power units), alongside benchmark alternatives including standalone combined heat and power unit (baseline), grid-dependent systems (without agrivoltaics), and off-grid agrivoltaic configurations. Results demonstrate that the on-grid 1-axis agrivoltaic system integrated with groundwater heat pump achieves superior techno-economic performance, delivering a net present value of 2.88 M€, representing a 4.1-fold improvement over conventional combined heat and power baseline systems. This configuration maximizes biomethane sales by electrifying thermal demands, avoiding biogas combustion and capitalizing on favorable biomethane-to-electricity price ratios. Heat pump electrification strategies consistently outperform biogas-combustion strategies (boiler or combined heat and power) in net present value, achieving up to 8.7 times higher performance through strategic biogas preservation for upgrading within the primary scenarios. Comparative analysis confirms the superior techno-economic and spatial performance of optimized on-grid systems, with 9.17–11.23 M€ higher net present value and 17–20 times lower land occupation than off-grid alternatives. Sensitivity analysis confirms the consistent superiority of on-grid 1-axis agrivoltaic systems paired with heat pumps, reflecting robust trade-offs between energy yield, cost, and land priorities. The developed framework offers a versatile approach for integrating renewable energy in agricultural systems, promoting a sustainable energy transition while maintaining agricultural productivity.

1. Introduction

The incorporation of renewable energy systems into small-scale agricultural activities, defined as farms occupying up to two hectares [1], is essential for advancing sustainability, mitigating greenhouse gas (GHG) emissions, and enhancing rural energy accessibility [2]. Among renewable solutions, biomethane ($BioCH_4$) production via anaerobic digestion (AD) of organic substrates offers substantial environmental and economic benefits, serving both as a renewable energy source and an effective waste management strategy [3]. Upgraded $BioCH_4$ is highly versatile, as it can be integrated into existing gas infrastructure or utilized directly in combined heat and power (CHP) plants and biogas boilers to address diverse energy requirements.

Previous studies have evaluated several renewable integration frameworks designed to boost energy self-reliance and economic viability. Temiz et al. [4] explored an integrated energy system in Thailand that combined overhead fixed bifacial agrivoltaic (APV) systems, biogas production units, and community-scale energy infrastructure, fully addressing local electricity, biogas, heating, and cooling demands. Similarly, Bambokela et al. [5] validated the dependability of hybrid mini-grid solutions integrating ground-mounted photovoltaic

* Corresponding author.
E-mail address: amirhossein.nikzad@unicatt.it (A. Nik Zad).

https://doi.org/10.1016/j.enconman.2025.120791
Received 22 August 2025; Received in revised form 17 November 2025; Accepted 18 November 2025
0196-8904/© 2025 The Author(s). Published by Elsevier Ltd. This is an open access article under the CC BY license (http://creativecommons.org/licenses/by/4.0/).

Nomenclature

A_{max}	Maximum available land area (m^2)
AD	Anaerobic Digestion
APV	Agrivoltaic
APV_t	Instantaneous APV energy conversion at time t
BESS	Battery Energy Storage Systems
$BioCH_4$	Biomethane
C_0	Initial cost of each equipment (€)
C_{cap}	Capital cost of components (€)
C_n	Nominal capacity of the battery (Ah)
$C_{O\&M}$	Operation and maintenance costs (€)
C_{PPG}	Costs of purchasing power from the national grid (€)
C_{rep}	Replacement cost (€)
CHP	Combined Heat and Power
COP	Coefficient of Performance
COP_{real}	Effective coefficient of performance of the heat pump
d	Discount rate (%)
E_{GWHP}	Hourly electrical energy consumed by GWHP (kWh_{el})
elecLoadt	Instantaneous electrical load at time t
EP_{APV}	Effective APV Penetration (%)
GWHP	Groundwater Heat Pump
i	Inflation rate (%)
INT	Integer Function
L_{comp}	Component's lifetime
L_{proj}	Project lifetime
L_{rem}	Remaining lifetime of the component at project end
LCC	Life Cycle Cost (€)
LCR	Life Cycle Revenue (€)
LHV_{Biogas}	Lower Heating Value of biogas (kWh/Nm^3)
MCDA	Multi-Criteria Decision Analysis
MOGA	Multi-Objective Genetic Algorithm
n	Year number or year of equipment replacement
N_{Batt}	Number of batteries required
NNSD	Number of Non-Sunny Days
$N_{PV,req}$	Total number of PV modules needed
NIS	Negative Ideal Solution
NPV	Net Present Value (€)
OH_{BGCHP}	Daily operating hours of the biogas CHP
OPEX	Operational Expenditures (€)
$P_{el,BiogasCHP}$	Electrical output of the biogas CHP (kW_{el})
$P_{PVmax,actual}$	Maximum output of each PV module (W)
$P_{th,BiogasCHP}$	Thermal output of the biogas CHP unit (kW_{th})
$P_{th,Biogasboiler}$	Thermal output of the biogas boiler (kW_{th})
PIS	Positive Ideal Solution
PSH	Peak Sun Hours
$Q_{BiogasCHP}$	Biogas availability for the CHP unit (Nm^3/day)
$Q_{Biogasboiler}$	Required biogas input rate for boiler (Nm^3)
Q_{GWHP}	Hourly thermal energy produced by the GWHP (kWh_{th})
R_{sal}	Salvage value of components (€)
R_{SBG}	Revenue from selling $BioCH_4$ (€)
R_{SPG}	Revenue from selling power (€)
SOC	State of Charge
T_{dig}	Digester operating temperature (°C)
T_{gw}	Groundwater temperature (°C)
TDL_{el}	Total daily electrical load (Wh)
TOPSIS	Technique for Order Preference by Similarity to Ideal Solution
V_n	Nominal voltage of the battery (V)

Greek symbols

α	Land occupation factor
$\eta_{el,Biogas\ CHP}$	Electrical conversion efficiency of the biogas CHP (%)
$\eta_{th,Biogas\ CHP}$	Thermal conversion efficiency of the biogas CHP (%)
$\eta_{th,Biogas\ boiler}$	Biogas boiler efficiency (%)
η_{r-t}	Roundtrip efficiency of the battery (%)

(GMPV) systems and biogas facilities for rural communities in Sub-Saharan Africa, underscoring the necessity for ongoing assessment of economic impacts across different configurations.

Further research into advanced hybrid technologies has highlighted specific economic challenges and opportunities. For instance, Sieborg et al. [6] analyzed biomethanation driven by GMPV integrated with a trickle bed reactor, indicating notable economic constraints for technology scale-up compared to conventional biogas upgrading methods. Conversely, Su et al. [7] demonstrated the promising economic prospects, and efficiency gains achievable through combining concentrated photovoltaic thermal (CPVT) collectors with AD processes, reporting a short payback period of approximately 5.6 years alongside significant reductions in fossil fuel dependency. Recent investigations have confirmed the effectiveness of integrating solar hybrid systems with AD units. For instance, Álvaro et al. [8] highlighted that hybrid photovoltaic thermal (PV/T) collectors can successfully supply both the heat and electricity required for biogas production and upgrading on isolated livestock farms, thereby reducing GHG emissions and enhancing farm energy self-sufficiency. Another study [9] focused on CPVT systems, demonstrating that their integration into a biogas plant improved annual biomethane production by 1.7 % and was economically feasible, achieving a positive net present palue (NPV) and a payback period of around 10 years. Calise et al. [10] assessed concentrating solar power (CSP) integrated with biogas facilities to satisfy both electrical and thermal energy demands, employing dynamic simulation using TRNSYS software. Their results indicated a substantial 45 % reduction in grid electricity reliance and 126 % savings in primary energy, coupled with a favorable payback period of six years, thus confirming the economic viability for transportation sector decarbonization. Additionally, Akarsu and Demir [11] conducted techno-economic and environmental analyses of biogas-based hybrid renewable systems for small livestock farms in rural Türkiye, concluding that a biogas-solar PV hybrid configuration integrated with the grid provided optimal performance, achieving a renewable energy fraction of nearly 90 %. Their study emphasized the critical role of governmental incentives in ensuring the financial feasibility of such renewable hybrid systems.

In the context of Italian agriculture, biogas generation stands out as a pivotal opportunity [12], providing the dual advantages of diversifying farm revenue streams and reinforcing sustainable agricultural practices [13]. Historically, the sector expanded under supportive renewable energy policies, beginning with the 2008 All-Inclusive Feed-in Tariff for small-scale plants, followed by revised incentive schemes in 2012 and 2016 [2]. This growth has positioned Italy among Europe's leading producers of upgraded biogas [3]. Currently, legislative frameworks and incentives are steering the sector toward biomethane production via biogas upgrading technologies [14], aligning with support measures under the REPowerEU framework [2]. However, the upgrading process required to convert raw biogas into biomethane is characterized by high energy consumption, creating a significant demand for auxiliary power [15]. Consequently, improving the energy efficiency of these facilities has emerged as a critical operational challenge. To address this energy demand and decarbonize the production chain, hybridizing AD infrastructure with APV systems represents a compelling renewable energy solution. Contemporary APV configurations have evolved to include diverse module designs, mounting structures, and tracking mechanisms tailored to various agricultural environments [16]. However, despite these advancements, integrated solutions combining biogas and solar energy, particularly APV systems, remain unexplored. Such integrated

systems offer significant potential to enhance overall sustainability and energy independence. Taramasso et al. [17] assessed four heat-power supply configurations for biomethane-producing AD plants in Italy, ranging from groundwater heat pumps (GWHP) powered by grid or GMPV electricity to CHP units supported by GWHPs or wood chip boilers. While combinations of GWHPs with PV generation proved economically attractive, achieving payback times of 4.2–4.8 years compared to 3.6–5.4 years for GWHPs powered by the grid, their analysis did not extend to the techno-economic optimization of APV systems.

Despite these advances, existing research has focused primarily on individual system components rather than integrated optimization frameworks that simultaneously evaluate multiple APV configurations with different heating technologies for biogas plants with a focus on $BioCH_4$ production. Additionally, systematic comparative analysis between on-grid and off-grid APV systems remains limited, particularly regarding the application of multi-objective optimization methods for APV-biogas integration strategies. The present research addresses these knowledge gaps by presenting a comprehensive optimization framework that evaluates the integration of biomethane production plant with various bifacial APV systems, which differ from conventional GMPV systems through greater pitch (row spacing) and elevated structures that allow continued farming. This study examines vertical and tracking (1-axis and 2-axis) APV configurations combined with supplementary energy sources, including biogas boilers, CHP units fueled by biogas, GWHPs, battery energy storage systems (BESS), and grid electricity. Methodologically, the framework explicitly accounts for key agronomic factors, such as row spacing, ground clearance, and tracker type, that influence both energy yield and land use in APV systems, thereby aligning energy-system design with crop management requirements.

The primary objective is to optimize grid-connected APV-biomethanation scenarios by applying the Technique for Order Preference by Similarity to Ideal Solution (TOPSIS) to results from a Multi-Objective Genetic Algorithm (MOGA) developed in MATLAB. To the best of current knowledge, there is no prior report of a combined and scenario-rich application in which a MOGA produces a portfolio of candidate solutions that is subsequently ranked using transparent Multi Criteria Decision Analysis (MCDA) with TOPSIS for the APV-biomethanation context. A techno-economic assessment is also conducted for alternative configurations, including biomethanation plant with a standalone biogas CHP unit (baseline), individual grid-based systems (without APVs), and off-grid APV systems, analyzed through analytical techno-economic evaluations to provide further insights. This analysis aims to establish the most economically viable configuration that ensures full coverage of the energy demands of an AD plant situated in Piacenza, Italy, over the project lifetime.

2. Materials and methods

This research explores energy strategies by integrating APV systems with a biogas plant producing an average of 125 Sm^3/h of $BioCH_4$. Considering APV limitations during night-time and unfavorable weather conditions, various scenarios are modeled to optimize energy performance and reliability. Each system component is sized according to the plant's electrical and thermal demands.

2.1. Description of the site and load profile

The mesophilic AD plant in Piacenza, Italy, operates at a constant temperature of 37 °C and incorporates membrane technology for biogas upgrading. The process involves biogas production from organic waste in the AD plant, followed by upgrading biogas into $BioCH_4$. Table S1 (Supplementary Material) reports the breakdown of feedstock materials in tons per hour. Summing these categories results in a total hourly intake of 4.75 tons (41,610 tons per year), corresponding to a weighted average specific heat of approximately 3.81 kJ/kg.K. Based on site-specific data [18], the plant produces 6789 normal cubic meters (Nm^3) of biogas per day, which, given a methane content of 54.2 %, corresponds to a daily $BioCH_4$ production of about 3680 Nm^3. A predominant fraction (75.95 %) of the total biogas output is upgraded to $BioCH_4$, while the remaining 24.05 % is fed into the CHP unit with a capacity of 150 kW_{el} (1633 Nm^3 biogas/day). Fig. S1 (Supplementary Material) illustrates the plant's annual electrical and heat demands at an hourly resolution. The total annual electricity demand is 1011.8 MWh_{el}, with a peak requirement of 119 kW_{el}. This demand covers the entire biogas production process including biogas compression, upgrading, and auxiliary systems. A detailed breakdown of the plant energy requirements is given in Table S2 (Supplementary Information). Note that electricity required by control electronics, motor starters, sensors, and cooling pumps associated with heat production units will be integrated into the overall electrical demand after system sizing. In contrast, the plant's heat demand of 1340 MWh_{th} shows considerable seasonal fluctuations, peaking at 179 kW_{th} in wintertime (January) and reaching its lowest levels during the summer.

2.2. Description of scenarios

This study evaluates eight scenarios designed to fully meet the thermal and electrical energy demands of the mesophilic AD plant in Piacenza. The analysis is structured around three primary on-grid APV scenarios (Scenarios 1–3), optimized using MOGA in MATLAB. These optimized scenarios are benchmarked against five alternative scenarios (Scenarios 4–8). Alternative scenarios assessed through analytical techno-economic evaluations, include a baseline case representing common industry practice (Scenario 4), two grid-dependent systems without APV integration (Scenarios 5–6), and two fully off-grid APV systems designed for energy autonomy (Scenarios 7–8). The terminology for these off-grid scenarios requires clarification. In the off-grid APV scenarios (S7-S8), the 'off-grid' designation applies exclusively to the electrical system. While the APV facility operates independently using battery storage, the biogas plant and upgrading unit maintain their connection to the gas grid for biomethane sales. These scenarios are representative of agricultural contexts where electrical grid interconnection is technically challenging or economically prohibitive, often due to remote siting. This configuration is contingent upon viable access to the gas grid or the feasible transport of biomethane via a virtual pipeline (i.e., truck transport). The analytical modeling of benchmark scenarios provides comparative insights into economic viability, performance, and trade-offs between optimized APV systems and conventional alternatives. All APV configurations utilize bifacial PV modules in three distinct setups including fixed vertical, overhead 1-axis, and overhead 2-axis tracking systems. The key components and energy supply strategies for all eight scenarios are summarized in Table 1.

A comprehensive schematic showing all the technological components and their potential interconnections, including heat, electricity, and biogas streams, is presented in Fig. 1.

2.3. Heat and electricity supply

The study adopts a heat load-following strategy, whereby heat producers are sized to fully meet the thermal demand of the AD plant,

Table 1
Summary of Evaluated Energy System Scenarios.

Scenario	APV	BESS	Grid	CHP	GWHP	Boiler
S1	✓	–	✓	–	–	✓
S2	✓	–	✓	–	✓	–
S3	✓	–	✓	✓	–	–
S4	–	–	–	✓	–	–
S5	–	–	✓	–	✓	–
S6	–	–	✓	–	–	✓
S7	✓	✓	–	–	–	✓
S8	✓	✓	–	–	✓	–

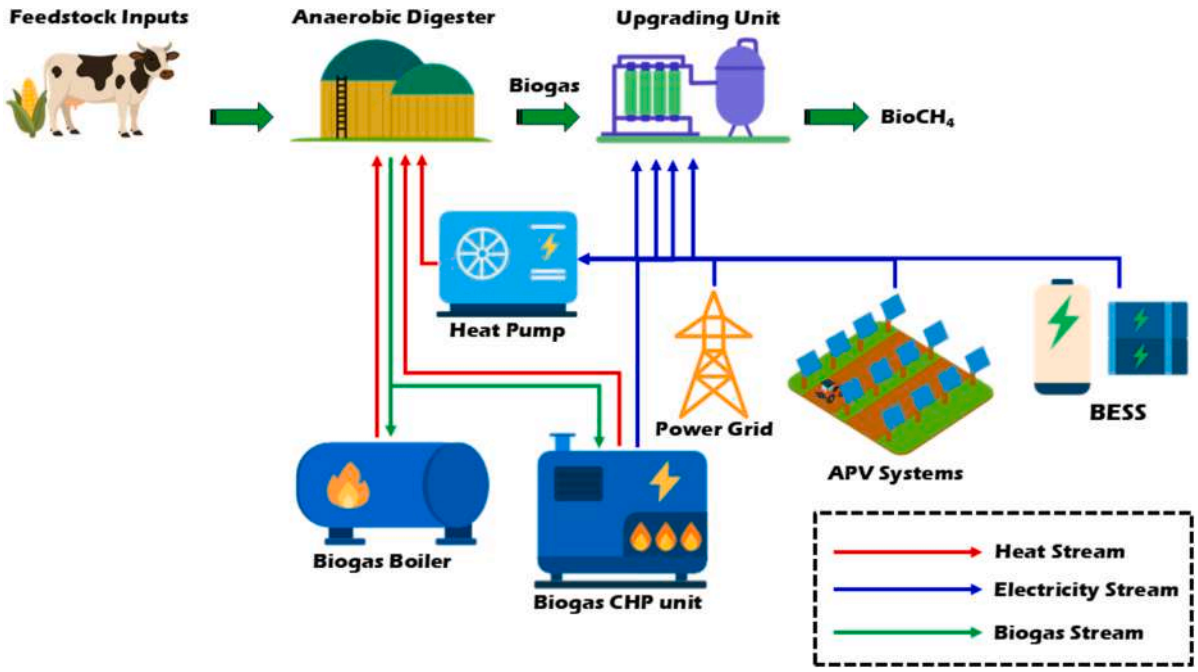


Fig. 1. Schematic of all involved equipment under investigation in this study.

ensuring stable digester operation. If an oversized heat producer is identified after sizing (probably due to the market availability), it is assumed that a system controller is implemented to modulate the heat producer's thermal output to exactly match hourly thermal demands, thus preventing excess heat production. Subsequent sections focus on the sizing criteria, selection process, biogas consumption (if applicable) and electrical energy requirements of the heat producers.

2.3.1. Biogas boiler

Biogas boilers burn biogas to generate thermal energy for uses like heating, drying, or preheating digesters. They offer environmental benefits from renewable fuel use but require careful design due to biogas variability and have higher initial costs than conventional boilers. In this study, the biogas boiler is sized based on the peak heat demand observed in January, measured at 179 kW_{th}. The lower heating value of biogas (LHV_{Biogas}) is assumed to be 5.5 kWh/Nm3, with the biogas boiler's efficiency ($\eta_{th,Biogasboiler}$) estimated at 85 % [19]. Given these parameters, the required biogas input rate can be calculated using Eq. (1) [19]:

$$P_{th,Biogasboiler} = Q_{Biogasboiler} \times LHV_{Biogas} \times \eta_{th,Biogasboiler} \quad (1)$$

where, $P_{th,Biogasboiler}$ represents the thermal output of the biogas boiler (kW_{th}), and $Q_{Biogasboiler}$ represents the required biogas input rate (Nm^3). Given that both the boiler efficiency and the LHV of biogas are predefined, the hourly biogas input rate is derived using Eq. (1). Finding a biogas boiler that precisely matches the peak thermal load (179 kW_{th} in January) poses challenges in the current market. As a result, the ATTSU RL-300 biogas boiler [20] with a maximum thermal output of 228 kW_{th} and 85 % efficiency was identified as a suitable option for this study. Since the selected biogas boiler has a higher thermal capacity than the actual peak demand, a system controller is assumed to regulate the boiler's biogas input rate. By adjusting the biogas flow rate according to hourly thermal demand, the boiler generates only the necessary heat, avoiding energy wastage despite its oversized nominal capacity.

The boiler's electrical demand mainly arises from its auxiliary components, such as pumps, fans, and control systems. By examining the catalogues, this consumption is estimated to be 1–2 % of the biogas boiler's thermal output, depending on the size of the boilers [20]. In this study, a conservative estimate of 1.5 % has been assumed. This auxiliary demand is covered within each scenario according to the respective energy supply configuration described in Section 2.2.

2.3.2. Heat pump

A heat pump is an energy-efficient system that transfers heat from external sources to meet heating demands. In this study, groundwater heat pumps (GWHPs) have been selected due to their stable groundwater temperatures year-round, enabling higher efficiency, particularly during colder months when heating demand peaks [17]. Compared to air-source heat pumps (ASHPs), GWHPs have higher initial installation costs associated with drilling and groundwater access; however, their superior efficiency results in lower operational costs, substantial long-term savings, and environmental benefits such as reduced GHG emissions, lower electricity usage, and minimal noise pollution [21]. Considering the peak heat demand and market availability, the Viessmann Vitocal 350 [22], with a maximum capacity of 181 kW_{th}, was selected as the most suitable option, closely matching the peak thermal requirement. Nevertheless, to ensure precise hourly heat delivery, the controller is assumed to modulate electrical input to the heat pump according to real-time heat requirements. Thus, the heat pump operates efficiently at varying partial loads, aligned exactly with the plant's hourly thermal demand. The hourly electrical power required for operating the GWHP is determined using Eq. (2) [17]:

$$E_{GWHP} = \frac{Q_{GWHP}}{COP_{real}} \quad (2)$$

In this expression, E_{GWHP} denotes the hourly electrical energy consumed by GWHP (kWh_{el}). Q_{GWHP} refers to the hourly thermal energy generated by the heat pump in kWh_{th}, which is set to exactly match the hourly heating requirement based on the heat load-following approach. The effective coefficient of performance (COP_{real}), a dimensionless indicator of the heat pump's efficiency in converting electricity into thermal energy, corresponds to 50 % of the theoretical COP obtained from the reversed Carnot cycle, as expressed in Eq. (3) [23,24]:

$$COP_{real} = 1/2 \times COP_{Carnot} = 1/2 \times \left(\frac{273.15 + T_{dig}}{T_{dig} - T_{gw}}\right) \quad (3)$$

where the digester temperature (T_{dig}) is maintained at 37 °C and the

groundwater temperature (T_{gw}) is set at 10 °C throughout the year, resulting in a calculated COP of 5.74. The COP directly determines the heat pump's electrical energy consumption through Eq. (2). With a calculated COP of 5.74, GWHP converts each kWh of electrical input into 5.74 kWh of thermal output. This electrical consumption is integrated into the plant's total electricity demand, which is then supplied by the configurations presented in Section 2.2.

2.3.3. Biogas combined heat and power unit

A biogas CHP unit converts biogas into electricity and heat simultaneously. Eq. (4) is utilized to calculate the rated heat capacity of biogas CHP unit [25]:

$$P_{th,BiogasCHP} = \frac{Q_{BiogasCHP} \times LHV_{Biogas} \times \eta_{th,BiogasCHP}}{OH_{BiogasCHP}} \quad (4)$$

where, $P_{th,BiogasCHP}$ (kW_{th}) represents the thermal output of the biogas CHP unit. $Q_{BiogasCHP}$, the biogas availability, is calculated as 24.05 % of biogas production as described previously, and $OH_{BiogasCHP}$ refers to the daily operating hours. These parameters were obtained through on-site assessments of the proposed biogas plant, as detailed in the Table S3 (Supplementary Material).

The thermal conversion efficiency of the biogas CHP unit, denoted as $\eta_{th,BiogasCHP}$, is assumed to be 50 %, for a small-scale biogas plant [26]. Eq. (5) is utilized to calculate the rated electrical capacity of biogas CHP unit [25]:

$$P_{el,BiogasCHP} = \frac{Q_{BiogasCHP} \times LHV_{Biogas} \times \eta_{el,BiogasCHP}}{OH_{BiogasCHP}} \quad (5)$$

where, $P_{el,BiogasCHP}$ (kW_{el}) represents the electrical output of the biogas CHP unit. The electrical conversion efficiency of the biogas CHP unit, denoted as $\eta_{el,BiogasCHP}$ is assumed to be 33 %, for a small-scale biogas plant [26]. Based on Eq. (4) and (5), the thermal and electrical outputs of the biogas CHP unit are 187.12 kW_{th} and 123.49 kW_{e1}, respectively, both of which fall within the range of the peak thermal and electrical demands. However, due to market availability, a biogas CHP unit with specifications closely matching the actual energy demand and efficiency requirements was selected, as shown in Table S4 (Supplementary Material) [27]. The selected biogas CHP unit has slightly higher heat

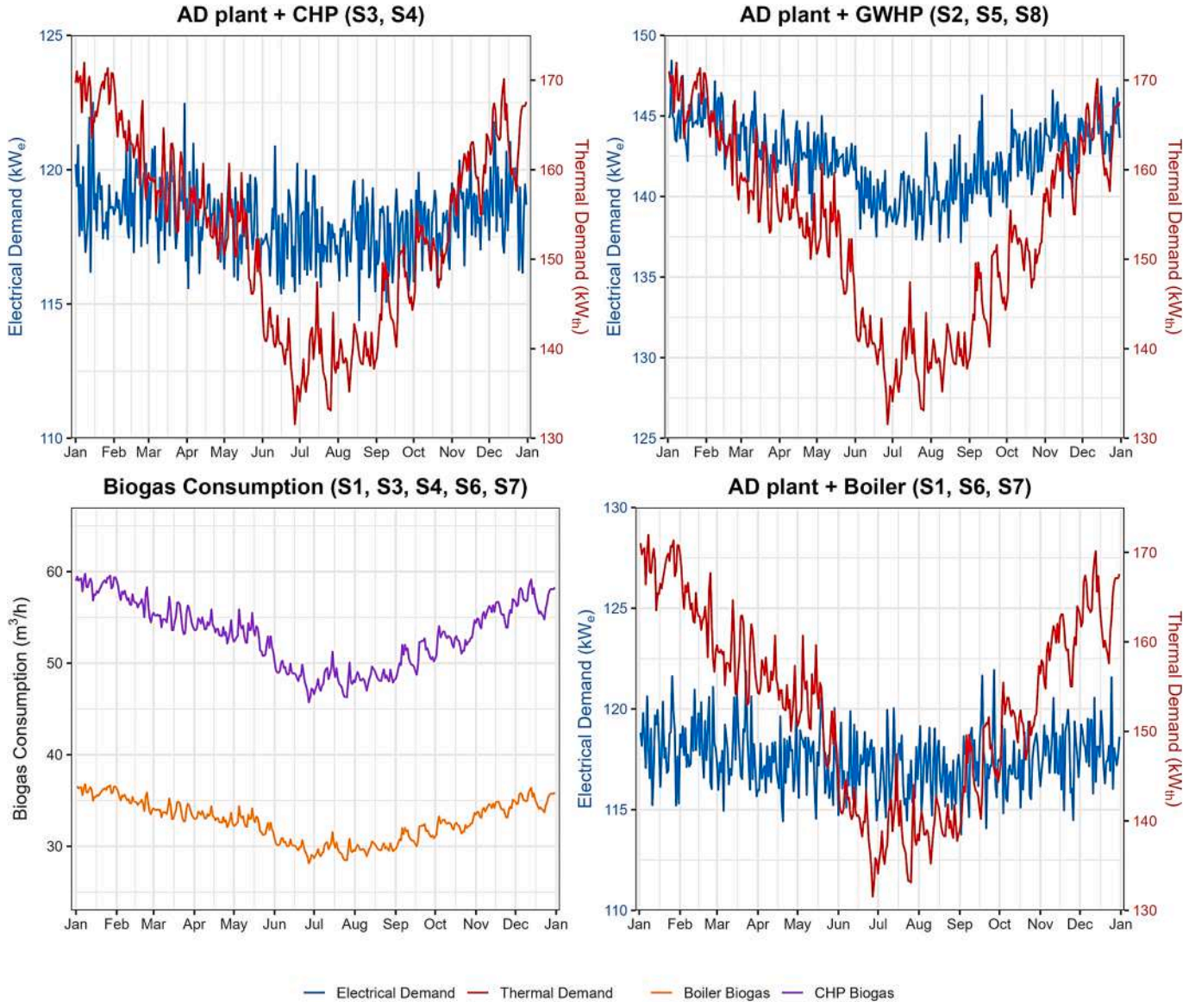


Fig. 2. Annual hourly profiles of AD plant energy demands and consumption in Piacenza. The electrical and thermal demand profiles are shown for systems using CHP unit (top-left), GWHP (top-right), and biogas boiler (bottom-right). The bottom-left panel details the hourly biogas consumption rates for the boiler and CHP unit scenarios.

capacity compared to the peak thermal load (179 kW_{th}). Consequently, a system controller is deployed to adjust biogas consumption hourly, ensuring the thermal output strictly corresponded to the actual thermal demand, preventing excess heat generation and reducing unnecessary biogas consumption. Using Eq. (4), the hourly biogas consumption of the CHP unit is calculated by equating its thermal output at each hour to the hourly thermal demand (heat load-following approach), divided by the product of the biogas LHV and the CHP's thermal efficiency. Once the hourly biogas input rates are determined through this procedure, the corresponding electrical output is calculated at each hour using Eq. (5). This component requires a continuous supply of electrical power to operate its auxiliary systems, including control electronics, sensors, and cooling pumps. This auxiliary consumption is assumed 3 % of the unit's electrical output [26]. Fig. 2 illustrates the plant's annual hourly thermal and electrical demands, including electricity consumed by heat generation units, as well as the hourly biogas consumption by the boiler and CHP units.

The total annual electricity demand of the AD plant varies depending on the heating technology employed, as detailed in Fig. 2. When incorporating a GWHP (top-right panel), the plant's annual electricity demand is highest at 1246 MWh_{el}, with a peak power requirement of 158 kW_{el}. In contrast, utilizing a CHP unit (top-left panel) results in an annual electricity demand of 1035 MWh_{el}, with a peak of 131 kW_{el}. Notably, the CHP unit generates 871 MWh_{el} annually when operated with the system controller. Employing a boiler system (bottom-right panel) leads to the lowest electricity demand at 1,029 MWh_{el}, with a peak of 130 kW_{el}. Regardless of the heating technology employed, the plant's total annual heat demand remains constant at 1340 MWh_{th}, consistent with the findings reported in [17], with a peak thermal demand of 179 kW_{th}. Concerning biogas use (bottom-left panel), the CHP unit uses a significantly higher volume, totaling 465,665 Nm^3 annually, compared to the boiler system, which consumes 286,521 Nm^3 per year.

2.4. On-grid agrivoltaic systems modeling

In this study, Agri-OptiCE® framework is employed to simulate and evaluate the hourly electricity production from three distinct APV system configurations. Agri-OptiCE® is an integrated simulation environment tailored to APV applications, extending a previously validated model [28,29] to account for a broader set of design variables and performance indicators. The framework integrates a solar irradiance and shading model that accounts for geometric layout and orientation, and a detailed PV performance model for bifacial modules. The resulting irradiance is converted to DC power using five parameter single-diode model with parameter extraction via the Newton-Raphson method, and subsequently to AC power through an inverter model, with losses such as mismatch also considered. These components simulate energy output based on irradiance conditions (including rear-side contributions), angle-of-incidence (AOI) effects, and temperature-dependent module efficiency. The simulation results have previously shown good agreement with field measurements and outputs from commercial software tools, providing confidence in the accuracy of this model [30]. The modeling framework employed for the simulations is outlined in the flowchart shown in Fig. 3, which is adapted from the procedure presented in [29].

In this study, three APV system configurations are simulated. The

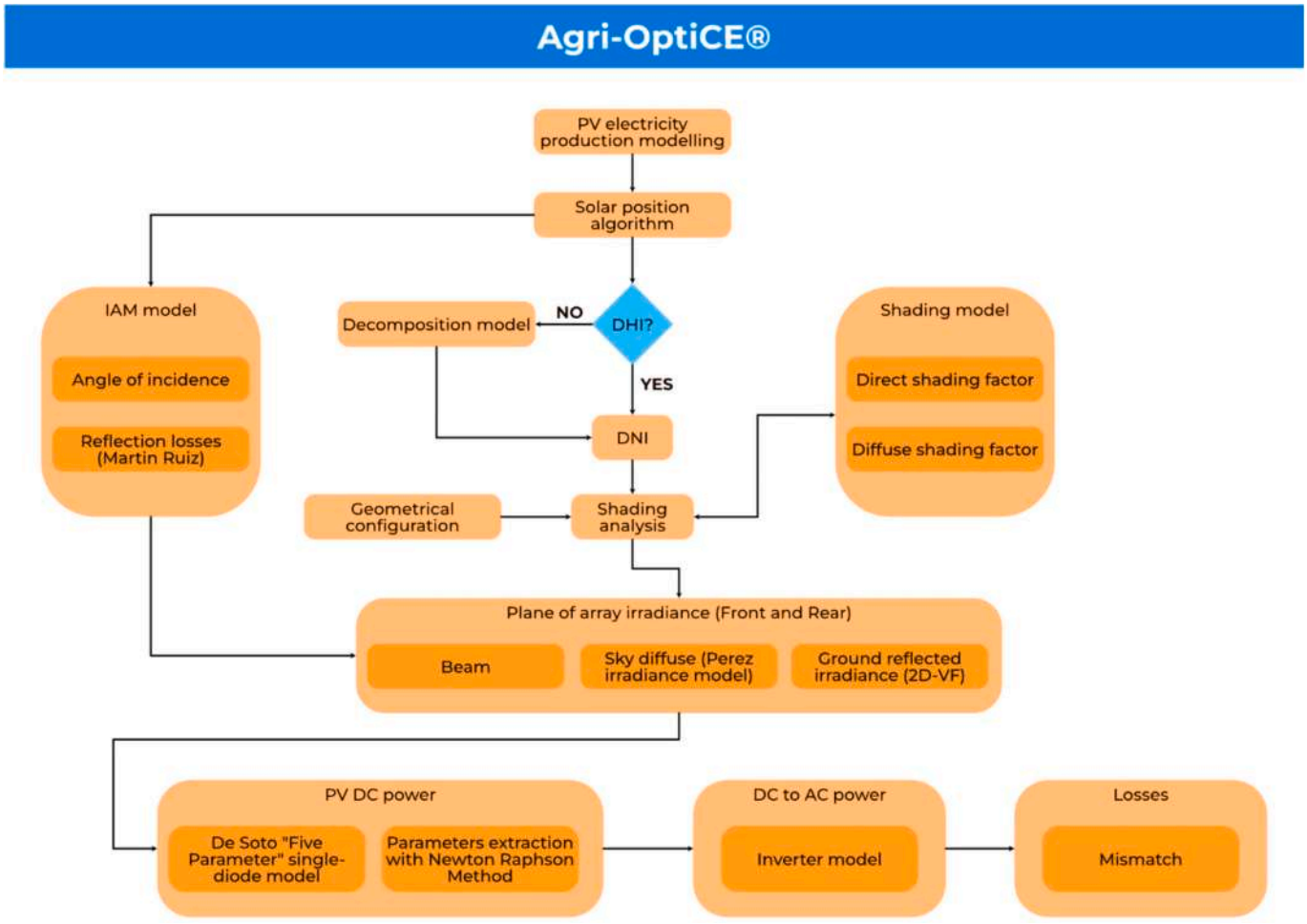


Fig. 3. Flowchart of the Agri-OptiCE® framework used in the simulation process [29].

system setups and input parameters used in the model are detailed in Table 2.

A distinct pitch between PV strings was evaluated for each APV system configuration, starting from a minimum allowable spacing, as outlined in [31]. While reduced pitch can improve land use efficiency, it was only considered when it did not obstruct agricultural machinery or introduce excessive PV self-shading. This approach ensures a careful balance between agricultural operability and energy performance. In practice, APV systems are also influenced by ground reflectance (albedo factor) from crops, but this aspect is beyond the scope of the present study. The hourly climate data used in the simulations were sourced from a nearby virtual weather station for the year 2019 [32], as illustrated in Fig. S2 (Supplementary Material).

In this year, the selected location recorded an annual global horizontal irradiance of 1370 kWh/m^2, an average temperature of 14.7 °C, and an average wind speed of 1.4 m/s. To reflect operational conditions, the simulations also include the characteristics of an on-grid inverter, as outlined in Table S5 (Supplementary Material).

2.4.1. Optimization problem

This section formulates the integrated on-grid optimization problem for scenarios 1−3 as a multi-objective problem. As described earlier, the entire heat demand of the AD plant is assumed to be fully met by the heat producers through the adoption of a heat-load-following approach. In the case of the CHP unit (Scenario 3), although the use of a system controller that regulates the biogas input based on hourly thermal demand ensures that all heat requirements are met, it also influences the unit's electricity production. Specifically, while the CHP operates at full load during winter due to high heat demand, it functions at partial capacity in summer when heat demand is significantly lower. As the system controller reduces the biogas input to match the reduced thermal needs, this also results in lower biogas input for electricity generation, thereby contributing to power deficits during those periods. Therefore, the optimization identifies the optimal combination of APV system type and capacity, along with the necessary contribution from the power grid, to fully meet the plant's electrical demand in the most cost-effective manner. The difference between the hourly electricity needs and the sum of the hourly electricity produced by the CHP and APV indicates the amount of electricity that needs to be drawn from the grid or the surplus electricity that can be injected into the grid. This value is crucial for the economic evaluation.

Table 2
Input data for simulation of energy output from different types of APV systems.

Parameters	Specifications
Location	Piacenza, 44.9744° N, 9.8924° E
Tracker max/min rotation angle	+55°/-55°
Height at rotation axis for 1-axis and 2-axis	5 *m*
Clearance for Vertical mounting system	0.7 *m*
Axis azimuth angle for 1-axis and 2-axis	South (0°)
Axis azimuth angle for Vertical	East (−90°)
PV array layout	6-Landscape (2-axis), 1-Portrait (1-axis), 2-Landscape (Vertical)
PV module	Trina solar, TSM-DEG21C-20
PV module nominal capacity	660 W_p
Efficiency	21.28 %
Bifaciality factor	75 %
Nominal operation module temperature	43 °C (±2°C)
Temperature co-efficient for P_{max}	− 0.34 %/°C
Number of cells	132 (66 × 2)
PV module dimension	2384 mm × 1303 mm × 35 mm
Albedo factor	0.25
Pitch between PV strings for 2-axis system	15 *m*
Module-to-module row spacing for 2-axis system	3.5 *m*
Pitch between PV strings for 1-axis system	6 *m*
Module-to-module row spacing for 1-axis system	1 cm
Pitch between PV strings for vertical system	8 *m*
Module-to-module row spacing for vertical system	1 cm

The objectives of the optimization are to maximize NPV, and to minimize the land occupation of the APV systems. NPV represents the difference between the present value of total project revenues and total project costs over the system lifetime, accounting for inflation and discount rates, as detailed in the economic modeling section. The decision variables include the type of APV system, represented as an integer variable that selects among vertical, 1-axis, and 2-axis configurations, and the installed capacity of the APV system in kilowatt-peak.

The problem is subject to two principal constraints that ensure realistic and sustainable operation. The first is a land-use constraint, stipulating that the product of installed capacity and the specific land area per kW_p (configuration-dependent) must not exceed 2 ha (20,000 m^2). This upper limit is consistent with the definition of small-scale agricultural holdings (≤2 ha) [1] adopted in this study, thereby aligning the system design with the intended application context. This constraint enforces the efficient use of available space. The second constraint concerns renewable energy penetration. In the boiler and heat pump scenarios, the effective APV penetration (EP_{APV}), defined as the proportion of the electrical load supplied by the APV system, must be at least 20 % to ensure a meaningful contribution from on-site renewables. In the CHP case (S3), the residual demand not met by the CHP unit is covered by APV and the grid, with the grid share limited to 50 %. The thresholds of 20 % and 50 % were adopted as pragmatic lower bounds. The 20 % requirement secures a tangible role for APV in hybrid systems, while the 50 % limit maintains on-site generation from CHP and APV as the dominant supply source without creating unrealistic operating constraints. This design choice ensures the feasibility of the optimization process while maintaining consistency with the study's focus on renewable energy integration. Finally, all annual costs and revenues are aggregated over the lifetime. The objective functions, constraints and decision variables are presented in the following subheadings.

2.4.2. Objective functions and constraints

The multi-objective optimization problem is formulated to minimize the objective vector J(x), which is defined as:

$$\min J(x) = [f_1(x), f_2(x)] \quad (6)$$

The individual objective functions, representing the economic and land-use performance criteria, are detailed below.

1. *Economic Performance (f_1):* The first objective is to maximize the project's financial return. This is achieved by minimizing the negative NPV, ensuring the selection of the most economically viable solution:

$$f_1(x) = -\mathrm{NPV} \quad (7)$$

2. *Land occupation (f_2):* The second objective is to minimize the land footprint of the APV installation. This is calculated as the product of the APV system's installed capacity and a technology-dependent land occupation factor

$$f_2(x) = x_2 \times \alpha \quad (8)$$

Here, x_2 represents the APV capacity in kW_p, and α is the specific land occupation factor (m^2/kW_p). Following [31], the value of α is influenced

by the APV system type, pitch, and PV module layout. In this study, $\alpha = 19.5\ m^2/kW_p$ is adopted for fixed vertical APV with 8 m pitch, $\alpha = 14.4\ m^2/kW_p$ for 1-axis tracking with 6 m pitch, and $\alpha = 20.95\ m^2/kW_p$ for 2-axis tracking with 15 m pitch (values aligned with Table 2).

2.4.3. Constraints

The optimization is governed by the following constraints:

1. *Land Area Constraint:* The total land area occupied by the APV system cannot exceed the maximum available agricultural land, A_{max}. This physical limitation is expressed as:

$$c_1(x) = (x_2 \times \alpha) - A_{max} \leq 0 \tag{9}$$

where, A_{max} is defined as 20,000 m^2.

2. *On-site Generation Constraint:* A minimum threshold for on-site electricity conversion must be met. The formulation of this constraint, $c_2(x)$, varies depending on the heating system configuration. For boiler and GWHP scenarios, it is assumed that at least 20 % of the annual electrical load must be satisfied by on-site APV electricity conversion. The constraint is formulated to ensure the energy conversion fraction meets this requirement:

$$c_2(x) = 0.2 - EP_{APV} \leq 0 \tag{10}$$

where EP_{APV} over an 8760-hour period is calculated through Eq. (11):

$$EP_{APV} = \frac{\sum_{t=1}^{8760} \min(APV_t,\ elecLoad_t)}{\sum_{t=1}^{8760} elecLoad_t} \tag{11}$$

In the equation above, APV_t is the instantaneous energy conversion by the APV system at hour t, and $elecLoad_t$ is the electrical load at hour t. For the CHP scenario, since the CHP unit already contributes to on-site generation, this constraint is modified to limit the grid dependency of the residual load. The fraction of the total load supplied by the grid, F_{grid}, must not exceed 50 %:

$$c_2(x) = F_{grid} - 0.5 \leq 0 \tag{12}$$

where F_{grid} denotes the ratio of net electricity imported from the grid to the total electrical load, as defined in Eq. (13):

$$F_{grid} = \frac{\sum_{t=1}^{8760} \max(elecLoad_t - APV_t,\ 0)}{\sum_{t=1}^{8760} elecLoad_t} \tag{13}$$

2.4.4. Decision variables

The optimization process is guided by the decision vector x, which includes one discrete and one continuous variable:

$$x = \begin{bmatrix} x_1 \\ x_1 \end{bmatrix}$$

where x_1 is APV system type. A discrete integer variable representing the technology choice: $x_1 \in [1, 2, 3]$, corresponding to vertical, 1-axis, and 2-axis systems, respectively. The APV system capacity, x_2, is a continuous variable representing the installed capacity of the APV system in kW_p. The search space is bounded as follows: $x_2 \in [1,1400]$. The upper bound is constrained by the maximum available land area (A_{max}) and the most land-intensive APV configuration (2-axis).

2.4.5. Optimization framework

The optimization framework in MATLAB loads scenario-specific MAT files containing hourly time series of electrical load, thermal demand, biogas consumption, and CHP electricity generation. This hourly input enables reliable modeling of energy flows, supports effective system sizing, and captures variability in operating conditions relevant for grid interaction [33,34]. Following data acquisition, simulation settings are defined by establishing a simulation period (8760 h) and setting decision variables. The next phase involves configuring the genetic algorithm (GA) with parameters including population size, generation count, mutation, and crossover rates. The GA solver is then executed using the described multi-objective functions. Within these functions, APV power output is obtained by loading kWh/kW_p profiles from Agri-OptiCE® and scaling them by candidate capacity. Scenario-specific calculations determine capital and operational expenditures (CAPEX, OPEX) as well as revenue streams. To evaluate long-term financial viability, the model applies discounted cash-flow factor that convert all future costs and revenues into present-value terms. This approach simultaneously accounts for inflation and the time value of money, ensuring that all monetary flows are consistently expressed in real terms suitable for NPV calculation. This evaluation framework supports the multi-objective optimization by integrating both technical performance and economic outcomes, providing a robust basis for comparing competing configurations and identifying the most cost-effective and revenue-enhancing design. The system economics are aggregated through these evaluations, culminating in a composite objective vector. Finally, a post-processing step employs TOPSIS ranking and candidate evaluation functions, which are discussed in the next section, to identify the optimal design candidate, which is then visualized through detailed metrics, specifically NPV and APV land occupation. Fig. 4 presents a detailed flowchart that illustrates the optimization process.

2.4.6. Procedure for TOPSIS-based candidate selection

To assess and rank the most suitable configurations for primary scenarios, we adopted a Multi-Criteria Decision Analysis (MCDA) framework based on results from a multi-objective optimization process. Among the available MCDA techniques, we selected TOPSIS for its capability to handle compensatory criteria and its widespread application in energy and environmental decision-making contexts [35,36]. TOPSIS is based on the idea that the optimal scenario should simultaneously show the shortest distance from a hypothetical Positive Ideal Solution (PIS) and the greatest distance from a Negative Ideal Solution (NIS), both defined by performance across a set of Key Performance Indicators (KPIs). Note that neither the PIS nor the NIS corresponds to an actual configuration; rather, they are theoretical constructs representing the best and worst observed performance values across all considered KPIs [37]. The method was applied by first constructing a decision matrix, where rows represented candidate configurations and columns corresponded to the two selected KPIs: NPV, to be maximized, and APV land occupation, to be minimized. To eliminate dimensional inconsistencies and ensure comparability, all KPI values were normalized using Min-Max scaling, transforming them to a common 0–1 range. A weighted-normalized matrix was then obtained by assigning a weight to each KPI according to its relative importance. In the primary analysis, equal weights (0.5 each) were assigned to the mentioned KPIs to maintain neutrality, avoiding subjective bias given the absence of specific stakeholder preferences or policy directives. For each configuration, the Euclidean distance to the PIS (D_i^+) and to the NIS (D_i^-) was calculated, and these two measures were synthesized into a Similarity Index (C_i) as follows:

$$C_i = \frac{D_i^-}{D_i^+ + D_i^-} \tag{14}$$

This index, ranging from 0 to 1, expresses the relative closeness of each configuration to the ideal solution. Higher C_i values indicate a better overall performance, representing a more favorable balance between maximizing NPV and minimizing APV land use. Configurations were then ranked in descending order according to their C_i scores.

To assess the robustness of the ranking, a sensitivity analysis was performed by varying the NPV weight (0.25, 0.50, and 0.75) while complementarily adjusting the weight of APV land occupation. This analysis illustrates how the rankings change under different stakeholder priorities, providing decision-makers with a broader understanding of

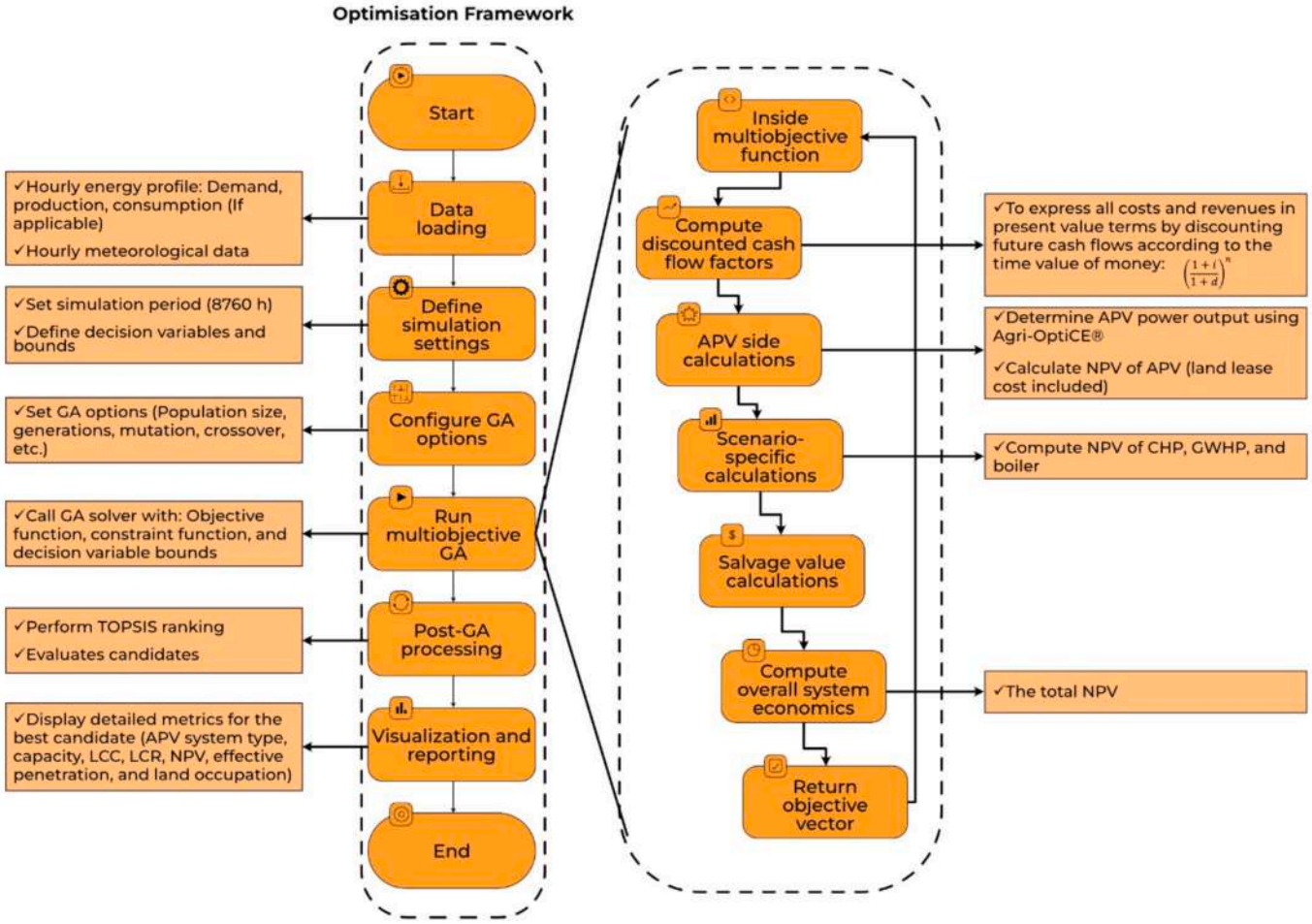


Fig. 4. Detailed flowchart explicitly illustrating the entire optimization process.

the trade-offs and stability of each configuration. The analysis was implemented using the Scikit-Criteria Python module [38], ensuring transparency and reproducibility.

2.5. *Off-grid agrivoltaic systems modeling*

In this section, three different off-grid bifacial APV systems (vertical, 1-axis, and 2-axis) are simulated using PVSOL® software [39], a comprehensive tool for designing, simulating, and analysing PV systems. PVSOL supports various off-grid PV configurations equipped with bifacial PV modules and enables performance modeling based on custom meteorological data and component specifications. To ensure consistency with the on-grid APV scenarios, all off-grid APV configurations were modeled using the same software assumptions (Table 2) and hourly meteorological data (Fig. S2). However, it is important to clarify the complementary roles of the simulation tools employed in this study. While Agri-OptiCE® provides APV performance baselines and crop-energy interaction modeling, it is not designed for off-grid applications. Commercial PV software such as PVSOL and PVsyst can simulate off-grid system performance effectively, but they do not inherently perform optimal component sizing based on detailed techno-economic constraints or load profiles. Typically, dedicated optimization tools such as HOMER Pro are required for techno-economic optimization; however, HOMER Pro directly lacks comprehensive support for bifacial PV modules, specific definitions of module height, pitch between PV strings, and the integration of custom hourly meteorological data. Additionally, PVsyst does not support the bifacial 2-axis configurations. Consequently, PVSOL was selected as the most suitable software since it supports all necessary configurations and custom data inputs. Nevertheless, component sizing, specifically the number of PV modules and battery banks, cannot be automatically sized within PVSOL. To overcome this limitation, a mathematical modeling was employed to accurately calculate the required number of PV modules and batteries. To determine the total required quantity of PV modules within the software, the following equation is employed [40]:

$$N_{PV,req} = \frac{TDL_{el} \times 1000}{PSH \times P_{PVmax,actual}} \tag{15}$$

where, $N_{PV,req}$ represents the total number of PV modules needed, TDL_{el} is the total daily electrical load (Wh), $P_{PVmax,actual}$ represents the maximum output of each PV module (W), factoring in system losses collectively referred to as the derating factor. This includes losses due to temperature, soiling, cabling, shading, module aging, and inefficiencies in batteries and inverters. The derating factor typically ranges from 0.7 to 0.8, with an average value of 0.75 assumed in this study [41]. PSH denotes the Peak Sun Hours, representing the period during which solar irradiation totals 1 kWh/m^2 on the PV module surface. For the specified location, the PSH values are calculated using PVSOL software.

In the off-grid scenarios, an annual capacity shortage of 0 % is set as a constraint, ensuring that the systems fully meet the entire electrical demand without interruption. This conservative approach is adopted to appropriately size the stand-alone APV capacity by explicitly considering the worst-case scenario of minimal solar availability. While this method may result in relatively large system sizes, it is essential to ensure uninterrupted operation under all seasonal and solar conditions. The off-grid inverter, essential for converting DC power from batteries to

AC, was sized using PVSOL software. The chosen model has an efficiency comparable to that of the on-grid inverter, ensuring fairness in the performance comparison. Technical specifications are given in Table S6 (Supplementary Material).

The battery banks ensure system reliability by storing energy to meet electricity demand during periods of low solar availability, such as cloudy conditions and nighttime. Surplus solar energy is stored in multiple battery units. The optimal number of batteries is determined using Eq. (16) [42]:

$$N_{Batt} = \frac{TDL_{el} \times NNSD}{C_n \times V_n \times \eta_{r\text{-}t} \times (1\text{-}\frac{SOC_{min}}{100})} \quad (16)$$

where, N_{batt} represents the number of batteries, TDL_{el} is the total daily electrical load (Wh), and NNSD refers to the number of non-sunny days per month (system autonomy days), assumed to be 3 [42]. C_n is the nominal capacity of a single storage unit (Ah), $\eta_{r\text{-}t}$ is the roundtrip efficiency (%), and V_n denotes the nominal voltage of a single storage unit (V). The minimum state of charge (SOC_{min}) is set at 20 %. The battery specifications selected by the software [43] are provided in Table S7 (Supplementary Material). It should also be noted that the dispatch of battery charging and discharging cycles, based on hourly load demands and solar irradiance variations, is performed by PVSOL. Key outputs from PVSOL simulations include total annual energy stored in batteries, annual surplus electricity generated, optimal off-grid inverter size, and missing energy (unmet load percentage). The calculation of APV land occupation follows the same approach as that employed for on-grid APV scenarios.

2.6. Economic modeling

The economic analysis for each scenario is performed by calculating the life cycle cost (LCC), life cycle revenue (LCR), and NPV. The NPV is defined as the difference between LCR and LCC, expressed in present value terms. A higher NPV indicates greater economic viability of the project. The life cycle cost represents the total expenses incurred over the lifetime of each component, discounted to present value by accounting for the time value of money. This includes the costs associated with initial investment, operation and maintenance costs (O&M), replacement costs, and the cost of purchasing electricity from the power grid. The LCC is calculated using the following equation [44]:

$$LCC = C_{cap} + C_{rep} + C_{O\&M} + C_{PPG} \quad (17)$$

where, C_{cap} denotes the capital cost of each component along with its installation costs (€), which is calculated using Eq. (18):

$$C_{cap} = C_{APV\ system} + C_{AD\ plant} + C_{Upgrading\ unit} + C_{battery\ packages} + C_{CHP\ unit} + C_{Biogas\ boiler} + C_{Heat\ pump} \quad (18)$$

C_{rep} includes the replacement cost of equipment at the end of its lifetime (€) and is calculated using Eq. (19) [45]:

$$C_{rep} = \sum_{n=1}^{N} C_0 \times \left(\frac{1+i}{1+d}\right)^n \quad (19)$$

where, C_0 is the initial cost of each equipment (€), i represents the inflation rate, d the discount rate, n the year of equipment replacement, and N the total project lifetime.

$C_{O\&M}$ (€) represents the total annualized costs, including operations and maintenance of all system components, feedstock, and land lease for the APV systems, and is calculated as follows [44]:

$$C_{O\&M} = \sum_{n=1}^{N} C_{O\&M,i} \times \left(\frac{1+i}{1+d}\right)^n \quad (20)$$

where, $C_{O\&M,i}$ represents the first-year operation and maintenance cost (€), and n denotes the number of year. It is assumed that all biogas fuel for the biogas boiler and CHP unit is supplied by the on-site biogas plant, eliminating the need for fuel price considerations.

C_{PPG} represents the costs associated with purchasing power from the national grid (€) over the project's lifetime, as indicated in Eq. (21) [44]:

$$C_{PPG} = \sum_{n=1}^{N} (\text{Annual electricity export} \times \text{unit price}) \times \left(\frac{1+i}{1+d}\right)^n \quad (21)$$

The LCR represents the total revenue generated over the project's lifetime from the sale of $BioCH_4$ to the gas grid, salvage value, and surplus electricity exported to the power grid, expressed in present worth. As given in [44], LCR is calculated using Eq. (22):

$$LCR = R_{sal} + R_{SPG} + R_{SBG} \quad (22)$$

The salvage value refers to the estimated residual value of a system component at the end of its useful life. According to [46], the salvage value is calculated using Eq. (23):

$$R_{sal} = C_{rep} \times \frac{L_{rem}}{L_{comp}} = \sum C_{rep} \times \frac{L_{comp}\text{-}(L_{proj}\text{-}(L_{comp} \times INT(\frac{L_{proj}}{L_{comp}})))}{L_{comp}} \quad (23)$$

where, R_{sal} refers to the salvage cost of all components (€), calculated based on linear depreciation, where the salvage value is proportional to the component's remaining life. L_{rem} indicates the remaining operational life of the component when the project ends, while L_{comp} represents the component's lifetime (years), and L_{proj} is the project lifetime, assumed to be 20 years. INT is a function that returns the integer value of a real number.

R_{SPG} and R_{SBG} represent the incomes from selling power back to the grid (€), and selling $BioCH_4$ produced to the gas grid (€) over the project's lifetime as indicated in Eq. (24):

$$R_{SPG} = \sum_{n=1}^{N} (\text{Annual electricity export} \times \text{unit price}) \times \left(\frac{1+i}{1+d}\right)^n$$

$$R_{SBG} = \sum_{n=1}^{N} (\text{Annual } BioCH_4 \text{ export} \times \text{unit price}) \times \left(\frac{1+i}{1+d}\right)^n \quad (24)$$

Finally, the NPV is calculated using Eq. (25) [44], applying the definition established in the Section 2.4.1:

$$NPV = LCR - LCC \quad (25)$$

In this study, the electricity purchase price from the grid and the feed-in tariff for grid injection in Italy were set at 0.20 €/kWh and 0.06 €/kWh, respectively [47]. To calculate the income from $BioCH_4$ sales, the annual biogas consumed by the biogas boiler and biogas CHP is subtracted from the total yearly biogas produced in the biogas plant. The remaining biogas, considering a methane content of 54.2 %, is then upgraded to $BioCH_4$ before being injected into the gas grid for sale. The revenue from $BioCH_4$ sales is 1.1 €/Nm^3 [18]. Additionally, an average inflation rate of 2 % and a discount rate of 6 % were applied, reflecting the economic conditions in Italy [48]. The lifespans assumed in this study were 20 years for the PV modules, heat pump, biogas boiler, AD plant, and biogas upgrading unit [17]; 10 years for solar batteries [47]; 7 years (60 K operating hours) for the biogas CHP unit; and 15 years for the solar inverter [49]. Components with lifetimes matching the project duration exhibit zero salvage value, while decommissioning costs are omitted under the assumption that these counterbalancing factors offset at project end. The CAPEX and OPEX associated with on-grid and off-grid APV components, heating systems, the AD plant, upgrading unit, feedstock, and land lease are detailed in Table S8 (Supplementary Material).

3. Results and discussion

This section presents the techno-economic results in three parts. It reports performance within the primary on-grid scenarios, examines economic drivers and sensitivities, and benchmarks outcomes against alternative configurations.

3.1. Primary scenarios

This subsection synthesizes scenario-level outcomes, clarifying the joint influence of on-grid APV configuration and heating technology on system performance. The principal drivers of the leading configuration are identified, and recurrent trade-offs across scenarios are highlighted.

3.1.1. Scenario-specific performance characteristics

The multi-objective optimization analysis was conducted for three on-grid energy integration scenarios to determine the optimal APV system configuration under varying energy demand profiles. Table 3 summarizes the techno-economic parameters of the evaluated scenarios, ranked by TOPSIS scores with equal weights assigned to all KPIs.

The results reveal substantial differences in economic and spatial performance among the tested configurations, offering critical insights for technology selection and investment prioritization. Scenario 2 (S2) demonstrates the most favorable economic performance, achieving the highest NPV range across all APV systems. The 1-axis APV system emerges as the most optimal configuration, delivering 173 kW_p of installed capacity with 22.46 % effective APV penetration while maintaining the highest TOPSIS score of 91.51. This superior performance is driven by its ability to achieve significant energy yield gains compared to vertical configurations, without incurring the high CAPEX penalties associated with 2-axis systems. In S2, the use of GWHP for digester heating eliminates direct biogas consumption for thermal supply, allowing a greater proportion of biogas to be upgraded to biomethane and sold to the gas grid. The economic advantage of heat pump electrification in S2 arises from two main factors. The high COP of 5.74 minimizes the electricity required for thermal production, and the preserved biogas maximizes the sales of high-value biomethane. This strategy reduces the opportunity cost associated with combustion-based options such as biogas CHP or boilers, where a significant share of biogas is diverted from upgrading to heat generation. The economic advantage of this approach is reinforced by the Italian market price differential between biomethane sales and electricity purchases from the national grid, reported to range from approximately 3.5 times in [17] to 5.5 times in the present study. Consequently, preserving biogas for upgrading yields a disproportionately greater impact on LCR, which is the primary contributor to NPV in the present analysis. Comparable results were reported in [17], where PV-powered GWHP systems achieved shorter payback periods and higher net revenues than CHP or boiler configurations under similar boundary conditions, thereby confirming the economic advantage observed for S2 in this study. Scenario 1 (S1) ranks second in overall performance, with NPV values ranging from 1 to 1.08 M€. The biogas boiler integration strategy shows moderate economic performance compared to GWHP integration (S2), primarily due to the opportunity cost of biogas consumption. While the biogas boiler itself has lower capital costs (€61,560 vs €107,229 for GWHP) and lower yearly O&M costs (€3,879 vs €5,090), its consumption of 11.6 % of total annual biogas production reduces the biomethane available for sale to the gas grid, resulting in 13 % lower LCR from biomethane sales compared to S2. Similar to S2, the 1-axis tracking system again demonstrates superior performance among the APV typologies in this scenario, achieving a 151 kW_p capacity and 23.74 % effective APV penetration, although its TOPSIS score (56.39) remains markedly lower than that of S2.

Scenario 3 (S3) yields the lowest economic returns, with NPVs clustered between 0.33 and 0.35 M€. The biogas CHP integration, while theoretically offering high efficiency through cogeneration, demonstrates limited economic advantages due to its consumption of 18.8 % of total annual biogas production, the highest among all scenarios. This substantial biogas consumption significantly reduces the biomethane available for profitable gas grid sales, resulting in the lowest overall economic performance despite the CHP's cogeneration benefits.

3.1.2. Technology-specific trade-offs

The comparative analysis across APV system types (Table 3) reveals consistent performance hierarchies within each scenario. 1-axis tracking systems consistently outperform both 2-axis and vertical configurations in terms of TOPSIS scores, demonstrating an optimal balance between energy yield, capital investment, and operational complexity. 2-axis tracking systems show intermediate performance, with higher energy yields partially offset by increased CAPEX and OPEX. The capacity reductions observed across scenarios (127 kW_p in S2, 104 kW_p in S1, 87 kW_p in S3) reflect the optimization algorithm's preference for cost-effectiveness over maximum energy capture under the given economic constraints. Vertical APV systems exhibit the lowest economic performance among the configurations examined. The present results indicate that they do not confer a land occupation benefit; rather, they require greater land area while delivering lower energy yields compared to tracking systems.

3.1.3. Economic analysis

The LCC analysis (Table 3) reveals distinct patterns across all on-grid APV scenarios. In S2, LCC values remain relatively stable across technologies, ranging only from 17.34 to 17.42 M€. This narrow spread indicates that total system costs in this scenario are only marginally affected by the APV configuration, meaning that economic performance is relatively insensitive to technology choice. By contrast, S3 shows the lowest LCC range (16.16–16.20 M€), which reflects reduced APV capacity requirements rather than inherent cost efficiency. The LCR patterns mirror the NPV trends, with S2 achieving the highest values (20.22–20.23 M€), followed by S1 (17.81–17.83 M€) and S3 (16.49–16.55 M€). This revenue hierarchy correlates directly with the effective APV penetration rates, highlighting the role of renewable energy integration in overall economic performance. Results indicating the economic advantage of 1-axis APV systems align with a broad body of literature conducted under diverse climatic conditions and methodological frameworks. For example, in the United States, a national techno-

Table 3
Main results across on-grid APV scenarios, ranked by TOPSIS scores.

Scenario	APV System Type	APV Capacity (kW_p)	EP_{APV} (%)	Land Occupation (m^2)	LCR (M€)	LCC (M€)	NPV (M€)	TOPSIS score
S2	1-axis	173	22.46	2489	20.22	17.34	2.88	91.51
S2	2-axis	127	20.05	2665	20.22	17.40	2.82	89.76
S2	Vertical	208	19.92	4055	20.23	17.42	2.81	83.31
S1	1-axis	151	23.74	2181	17.83	16.75	1.08	56.39
S1	2-axis	104	19.93	2185	17.81	16.80	1.01	55.43
S1	Vertical	171	19.91	3343	17.82	16.82	1.00	52.43
S3	1-axis	112	7.94	1607	16.55	16.20	0.35	50.01
S3	2-axis	87	7.96	1815	16.53	16.19	0.34	49.56
S3	Vertical	113	7.95	2208	16.49	16.16	0.33	48.72

economic assessment reported 1-axis APV system outperforming static layouts [44]. In Belgium, a head-to-head field comparison of vertical, fixed-elevated, and 1-axis designs found the 1-axis APV setup delivered the lowest levelized cost of electricity (LCOE) [49]. In the Italian context, Agostini et al. [50] found that 1-axis APV systems outperformed both fixed-tilt and 2-axis designs in cost-effectiveness, as the additional energy yield from 2-axis did not compensate for its higher CAPEX and OPEX. Bellone et al. [31], in an Italy-wide simulation of various APV configurations across five sites including Piacenza, applied an MCDA integrating energy conversion per hectare and CAPEX. Their results ranked the 1-axis configuration highest in TOPSIS score, followed by 2-axis and vertical systems, thereby corroborating the superior economic and technical viability of 1-axis APV systems under comparable constraints. A cross-country Monte Carlo analysis encompassing Sweden, Denmark, Germany, and Italy confirmed that 1-axis APV systems are the most profitable configuration, achieving approximately 20–30 % lower LCOE and shorter payback periods compared with vertical and elevated designs [51]. Multi-objective water-energy-food (WEF) nexus optimizations likewise consistently identify the 1-axis APV configuration as the most robust solution, balancing energy yield, crop performance, and irrigation water demand under diverse policy scenarios [52]. Additional Belgian field evidence further substantiates the technical and economic advantages of 1-axis APV systems, attributable to their higher energy conversion and more favorable LCOE [53].

3.1.4. Sensitivity analysis

The sensitivity analysis examining the impact of NPV weight variations on TOPSIS scores reveals critical insights into the robustness of decision-making frameworks and the relative importance of economic versus technical criteria in APV systems optimization. The analysis systematically varies the NPV weight (ω) from 0 to 1 while maintaining proportional adjustments to APV land occupation weights, providing a comprehensive assessment of decision stability across different priority structures. Fig. 5 presents the TOPSIS scores for primary scenarios (S1-S3), illustrating the trade-off between land occupation and NPV across all APV configurations including vertical (1), 1-axis tracking (2), and 2-axis tracking (3), under NPV weightings of 0.25, 0.5, and 0.75.

Notably, S2 (GWHP configuration) consistently ranks highest in TOPSIS scores across all weightings, driven mainly by its superior NPV compared with S1 (biogas boiler configuration) and S3 (CHP configuration). This indicates that the higher NPV in S2 dominates the decision space and cannot be offset by land occupation trade-offs in the other scenarios. This effect is particularly evident in S3, where TOPSIS scores remain consistently below 51 across all weightings, indicating that even its relatively compact land footprint cannot compensate for the economic penalties associated with high biogas consumption for CHP operation. Regarding the APV system types, 1-axis tracking systems tend to require less land while delivering the highest NPVs, explaining why the multi-objective optimization often converges on these configurations. In contrast, vertical APV systems generally require more land to achieve comparable NPVs, due to their lower specific energy yields. Importantly, the TOPSIS analysis reveals that increasing the weight on NPV (from $\omega = 0.25$ to $\omega = 0.75$) progressively enhances the relative performance advantage of S2. This indicates that economic prioritization tends to amplify the superiority of configurations that maximize biomethane sales revenue. Conversely, when more weight is placed on land occupation ($\omega = 0.25$), the performance differentials between scenarios narrows slightly, though S2 retains its dominant position, highlighting both the robustness of the GWHP-based strategy and the sensitivity of optimal rankings to decision-maker preferences regarding spatial versus economic objectives.

3.2. Alternative scenarios

Five alternative configurations (S4-S8) were evaluated through analytical techno-economic evaluation to benchmark their performance against the optimized on-grid APV cases for further insights. These include a baseline CHP only system (S4), two grid-based options (S5 and S6), and two off-grid APV systems (S7 and S8). All configurations were designed to meet the complete electrical and thermal demands of the AD plant. Off-grid scenarios utilize a biogas boiler in S7 and a GWHP unit in S8. System sizing for two off-grid APV systems was determined using a mathematical modeling framework (as previously described in the methodology) and operational performance was simulated in PVSOL. Key results for these two scenarios are presented in Table 4.

Results indicate that the 2-axis APV system, due to advanced tracking technology, requires up to 26.35 % fewer PV modules, total capacity, and inverter size compared to the 1-axis system in both scenarios. Conversely, the vertical APV system, due to its fixed orientation without tracking, necessitates the highest number of PV modules to sufficiently charge the batteries. Interestingly, despite using more PV modules, the vertical system generates less surplus electricity than the 1-axis system, though still more than the 2-axis system. This variation arises from differences in system capacities and technological efficiencies. Across all

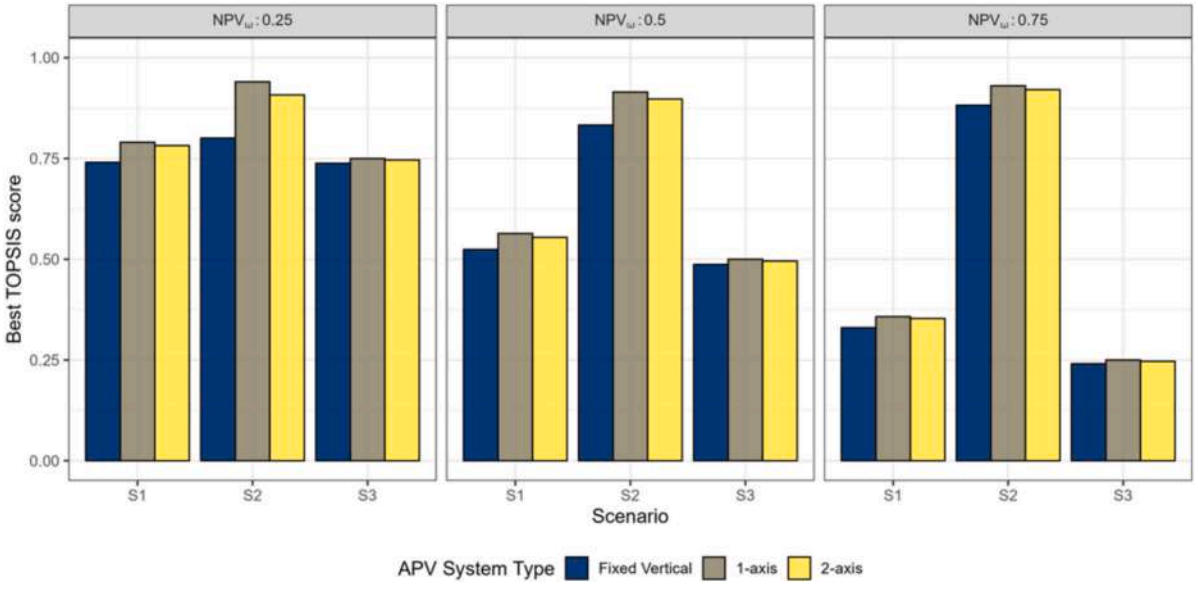


Fig. 5. Sensitivity analysis of TOPSIS scores to NPV weight variations (0.25, 0.5, and 0.75) across primary scenarios.

Table 4
Sizing and Performance Comparison of Off-grid APV Systems for S7 and S8.

Description	APV system type in S7			APV system type in S8		
	Vertical	1-axis	2-axis	Vertical	1-axis	2-axis
Total PV modules	4155	3908	2878	5537	5207	3835
Total Capacity (MW_p)	2.74	2.58	1.9	3.65	3.43	2.53
Off-grid Inverter Size (MW_p)	2.4	2.26	1.67	3.21	3	2.21
Total Batteries		851 for S7			1130 for S8	
Total energy stored in batteries (MWh)		11.03			14.64	
Unmet load (%)	<2	<1	<1	<3	<2	<2
	Pitch 8 *m*	Pitch 6 *m*	Pitch 15 *m*	Pitch 8 *m*	Pitch 6 *m*	Pitch 15 *m*
Land occupation (ha)	5.35	3.72	3.98	7.13	4.95	5.3
Annual surplus electricity (MWh)	2265	2709	2058	3135	3681	2724

evaluated metrics, S8 consistently presents higher values compared to S7, primarily due to the significantly greater electrical demand of the GWHP relative to the biogas boiler. Consequently, S8 demands substantially more PV modules, increased battery capacity (1130 compared to 851 batteries), and greater total battery storage capacity (14.64 MWh versus 11.03 MWh). These substantial quantities of PV modules and batteries stem from the fact that, in the sizing procedure for the off-grid APV systems, a 0 % annual capacity shortage constraint was imposed to guarantee uninterrupted fulfillment of the total electrical demand. The resulting unmet load remains very low across all configurations (below 3 % in all cases) demonstrating that the adopted sizing approach effectively meets the target reliability criteria. The 1-axis and 2-axis systems achieve the lowest shortfalls, reflecting their higher conversion efficiency and better alignment of generation with demand profiles. The slightly higher unmet load of the vertical systems, despite their greater installed capacity, is attributable to reduced production during low-sun periods when battery discharge is insufficient to fully meet instantaneous loads. In terms of land occupation, the vertical APV system requires the largest area, attributable to its higher PV module count and installation requirements. The 1-axis system remains the most space-efficient due to its smaller pitch. The 2-axis system, despite employing larger pitch spacing, occupies less land area than the vertical configuration due to fewer required PV modules, enabled by its advanced tracking capability. This makes the 2-axis system ideal for minimizing land use at greater pitches, whereas the 1-axis system is preferable for tighter spatial configurations. Nevertheless, considerations such as installation and maintenance costs should also influence final system selection.

In the grid-based alternatives, the Italian national power grid fully supplies the annual electrical demand. As indicated in Fig. 2, the AD plant integrated with a GWHP (S5) has a total annual electricity demand of 1246 MWh_{el}, whereas using a biogas boiler (S6) reduces this demand to 1029 MWh_{el}. Regardless of the heating technology implemented, the plant's total annual heat demand remains constant at 1340 MWh_{th}.

In the baseline scenario, CHP operation without complementary generation sources imposes constraints on energy output control. Implementing a system controller in this particular scenario is not feasible because the CHP unit operates independently. Adjusting the CHP's power input to align its thermal output with monthly heat demands would consequently alter its electrical output. Since there is no additional electrical generator in this scenario, employing a controller is impractical. As a result, the selected biogas CHP unit generates electrical and thermal outputs exceeding the actual plant demands, resulting in an excess of 44 MWh_{el} electricity and 554 MWh_{th} heat annually. In this study, excess electricity is assumed to be exported to the power grid to generate revenue, while excess heat, due to the absence of control system, is considered wasted. In line with current policy frameworks, which prioritize upgrading biogas to $BioCH_4$ for grid injection or transport applications over heat production [54], stakeholders are incentivised to minimize on-site biogas use. This can involve replacing CHP units or biogas boilers with heat pumps, or combining them with APV systems. Finally, Table 5 presents the economic evaluation of all alternative scenarios over the project's lifetime, ranked by NPV as a benchmark for economic performance.

The economic evaluation of the alternative scenarios reveals substantial performance disparities, clearly distinguishing the viability of grid-connected versus off-grid configurations. The results, summarized in Table 5, indicate that all off-grid APV systems (S7 and S8) are economically unfeasible under the current financial assumptions, yielding significantly negative NPV ranging from −6.27 M€ to −8.33 M€. This outcome is driven by a combination of the extremely high LCC associated with these systems (ranging from 25.47 M€ to 30.31 M€) and the inability to generate revenue from surplus electricity. The high LCC reflects the extensive capital investment required for large-scale APV arrays and battery storage systems sized to guarantee complete energy autonomy. Furthermore, a substantial amount of electricity conversion by off-grid APV systems is wasted as it cannot be sold to the grid, representing a significant loss of potential revenue. In terms of land-use intensity, off-grid systems occupy substantially more land than their optimized on-grid counterparts across all APV typologies, typically ranging from 17 to 20 times higher. The greatest land occupation occurs in the vertical configuration, where the off-grid system (S8) requires 7.13 ha compared with 0.41 ha in its optimized on-grid counterpart, confirming the superior land-use efficiency of optimized on-grid APV systems. Comparing the two off-grid approaches, the scenarios utilizing a GWHP (S8) result in lower NPV than those with a biogas boiler (S7). This is because the higher electrical demand of the GWHP necessitates an even larger and more costly APV and battery installation, further inflating the LCC and exacerbating the economic deficit. S8 also exhibits lower spatial efficiency than S7 due to its larger installed capacity and consequently greater land requirement. In sharp contrast, the grid-based scenarios demonstrate positive economic returns. S5 (Power grid + GWHP) emerges as the most profitable alternative, achieving a robust NPV of 2.41 M€. Its strong performance is attributed to a high LCR of 20.22 M€, generated by upgrading and selling the entire volume of biogas as biomethane. This configuration avoids the prohibitive costs of energy storage while maximizing the primary revenue stream. S6 (Power grid + biogas boiler) is the second most profitable among the grid-based options, with an NPV of 0.72 M€, as it diverts 11.6 % of the total biogas production for thermal energy, thereby lowering its LCR compared to S5. Finally, the baseline scenario, S4 (Biogas CHP unit), ranks as the third-most viable alternative with an NPV of 0.70 M€. Despite having the lowest LCC (15.78 M€), its profitability is constrained because the on-site consumption of 18.8 % of the total biogas reduces potential biomethane sales revenues.

Crucially, a comparative analysis establishes that the optimal primary scenario identified through multi-objective optimization (S2: 1-axis APV system paired with GWHP) remains the most financially advantageous solution overall. With an NPV of 2.88 M€ (from Table 3), the S2 configuration outperforms the best alternative scenario (S5) by approximately 20 %. Both S2 and S5 leverage the GWHP to maximize biomethane revenue, resulting in identical LCR. However, the

Table 5
Summary of the economic evaluation results for the alternative scenarios.

Scenario	Configuration	APV System Type	LCR (M€)	LCC (M€)	NPV (M€)
S5	Power grid + GWHP	None	20.22	17.81	2.41
S6	Power grid + biogas boiler	None	17.88	17.16	0.72
S4 (baseline)	Biogas CHP	None	16.48	15.78	0.70
S7	Off-grid APV + biogas boiler	Vertical	19.20	25.47	−6.27
	Off-grid APV + biogas boiler	2-axis	19.19	25.87	−6.68
	Off-grid APV + biogas boiler	1-axis	19.21	26.30	−7.09
S8	Off-grid APV + GWHP	Vertical	21.97	29.19	−7.22
	Off-grid APV + GWHP	2-axis	21.96	29.73	−7.77
	Off-grid APV + GWHP	1-axis	21.98	30.31	−8.33

superiority of S2 stems from its lower LCC (17.34 M€ vs. 17.81 M€ for S5). This cost advantage is achieved because the integrated APV system in S2 reduces the reliance on purchasing electricity from the grid over the project's lifetime. However, when viewed through the lens of energy sustainability and resilience, other primary scenarios (S1 and S3) present notable advantages over S5, despite their lower NPV. S5 relies entirely on the national grid for its electricity supply, whereas S1 and S3 incorporate significant shares of on-site renewable generation, with effective APV penetrations of over 20 %. The case for S3 is particularly compelling from a sustainability standpoint; although it has a lower APV penetration (7.9 %), approximately 84.1 % of its total electrical demand is met by the biogas CHP unit. Consequently, only about 8 % of its electricity is drawn from the grid, compared to 100 % in S5. This highlights a critical trade-off between pure economic optimization and the promotion of decentralized, renewable energy systems. This analysis confirms that the synergistic integration of an on-site APV system, as achieved in the optimized scenarios, yields a more profitable outcome than any of the evaluated fixed-alternative configurations, while also offering pathways to enhanced energy sustainability.

3.3. Study limitations and future directions

As a first attempt to integrate APV systems with biomethanation in a unified techno-economic optimization framework, this study presents several limitations that offer opportunities for future research development. The scope is deliberately constrained to techno-economic optimization of integrated APV-biomethanation systems, focusing exclusively on electrical energy output without agricultural yield modeling. While agrivoltaic terminology is employed due to the agricultural land context, the primary contribution lies in energy system optimization rather than agronomic analysis. Future research should integrate detailed crop yield models to quantify food-energy trade-offs within the water-energy-food nexus framework.

Energy yields are simulated using fixed derating factors, module temperature coefficients, and representative meteorological inputs. Single-year weather files and constant albedo parameters may underrepresent interannual variability, seasonal surface changes, and degradation effects, which can influence hourly matching and annual energy conversion. Multi-year ensembles, dynamic albedo modeling, and explicit degradation trajectories would narrow these uncertainties and propagate more faithfully to economic indicators.

Economic conclusions depend on price and policy parameters. CAPEX and OPEX, grid tariffs/feed-in conditions, biomethane prices, land lease cost, and discount/inflation rates are treated as fixed parameters within each scenario. Because these drivers are volatile and policy-contingent, a stochastic cash-flow analysis (e.g., Monte Carlo on prices/incentives) would better characterise risk to LCOE, NPV, and payback and identify thresholds at which the preferred configuration changes.

Sizing and operational assumptions also affect performance. Off-grid designs are dimensioned to achieve zero annual capacity shortage, which ensures reliability but is conservative and capital-intensive. Allowing a small loss-of-load (LOL) probability, co-optimising battery/inverter ratings with demand response, or integrating thermal storage could materially reduce required PV and storage. Likewise, fixed pitch and simplified supervisory control may not capture the attainable benefits of advanced tracking and dispatch; variable-pitch optimization and enhanced control policies could further improve both economics and land use. Additionally, the analysis assumes mesophilic digestion at 37 °C, though thermophilic operation (50–60 °C) would increase thermal demand, potentially favouring biogas combustion over heat pump electrification due to reduced heat pump efficiency at higher temperature lifts. Equipment selection was based on capacity matching and market availability rather than comprehensive market surveys, which may not fully represent efficiency ranges or cost structures across broader market conditions. Future studies could incorporate multiple manufacturer options or equipment sensitivity analysis to assess robustness across diverse market scenarios.

The present analysis emphasizes cost, performance, and land occupation. A parallel LCA has recently quantified the environmental burdens of these configurations, highlighting that material-intensive systems like 2-axis APV systems incur higher carbon footprints despite their energy gains; while 1-axis APV configurations offer superior environmental performance, achieving the lowest GHG emissions due to optimized material efficiency [55]. Future research should strictly link these techno-economic models to LCA and crop models to enable comprehensive MCDA that balances financial returns with environmental sustainability and resource efficiency.

Finally, several insights are transferable. First, electrification via heat pumps paired with APV tends to outperform combustion routes when upgraded biomethane commands a premium. Second, 1-axis APV frequently captures most tracking benefits at lower CAPEX and OPEX than 2-axis, making it a robust compromise across policy settings. Third, decision robustness improves when alternatives are ranked with explicit trade-off tools such as TOPSIS and when weight and price sensitivity are tested; these elements are readily reusable for other integrated agro-energy systems.

4. Conclusion

This study presents the first optimization framework integrating bifacial APV systems with an anaerobic digestion plant for biomethane production, employing a multi-objective genetic algorithm coupled with the TOPSIS methodology to identify optimal energy configurations. Key findings demonstrate that the optimized on-grid APV configuration combining 1-axis tracking paired with GWHP (S2) achieves superior economic performance with an NPV of 2.88 M€, outperforming the conventional CHP baseline by 4.1 times. The economic advantage arises from strategic thermal-demand electrification, avoiding biogas combustion to maximize high-value biomethane sales, achieving up to 8.7 times higher NPV compared with combustion-based strategies within the primary scenarios. The 1-axis tracking systems consistently provided the most balanced trade-off between energy yield and cost-effectiveness across all configurations. Comparative analysis shows that off-grid APV systems incur substantially higher LCC (25.5–30.31 M€) than LCR (19.2–22 M€), leading to negative NPVs, while optimized on-grid

systems maintain balanced revenues and costs, resulting in positive economic outcomes and 17–20 times lower land occupation across all APV typologies. These results underscore the critical role of grid connection in ensuring sustainable profitability and spatial efficiency. Electrifying anaerobic-digestion thermal loads via APV-powered heat pumps emerges as a robust decarbonization strategy that enhances biomethane-plant profitability. The consistent superiority of 1-axis tracking systems indicates technological maturity suitable for standardization and large-scale deployment, emphasizing the importance of site-specific, integrated optimization to maximize hybrid renewable-energy potential while maintaining efficient dual land use.

Declaration of Generative AI and AI-assisted technologies in the writing process

During the preparation of this work the authors used ChatGPT (OpenAI) in order to assist in refining the language and improving the readability of the manuscript. After using this tool/service, the authors thoroughly reviewed and edited the content as needed and take(s) full responsibility for the content of the publication.

CRediT authorship contribution statement

Amirhossein Nik Zad: Writing – review & editing, Writing – original draft, Visualization, Validation, Software, Methodology, Investigation, Formal analysis, Data curation, Conceptualization. **Sebastian Zainali:** Writing – review & editing, Writing – original draft, Visualization. **Michele Croci:** Writing – review & editing, Visualization, Software. **Mohammed Guezgouz:** Writing – review & editing. **Giorgio Impollonia:** Writing – review & editing. **Pietro Elia Campana:** Writing – review & editing, Writing – original draft. **Stefano Amaducci:** Writing – review & editing, Writing – original draft, Supervision, Methodology, Investigation, Funding acquisition, Formal analysis, Conceptualization.

Declaration of competing interest

The authors declare the following financial interests/personal relationships which may be considered as potential competing interests: The company European Energy is financing half of Sebastian Zainali's Ph.D. salary.

Acknowledgements

Funded by the European Union (project 101116076—VALUE4FARM). Views and opinions expressed are, however, those of the author(s) only and do not necessarily reflect those of the European Union or the European Climate, Infrastructure, and Environment Executive Agency (CINEA). Neither the European Union nor the granting authority can be held responsible for them. Amirhossein Nik Zad was supported by the PhD in Agro-Food System (Agrisystem) and by Portus project funded by Romeo and Enrica Invernizzi Foundation. Michele Croci was partially supported by "National Research Centre for Agricultural Technologies (Agritech)" CN00000022.PNRR-M4C2, Investment 1.4—Funded by the European Union— NextGenerationEU'—CUP: J33C22001160007. Financial support was also received from the Swedish Energy Agency through the project "The Solar Electricity Research Centre (SOLVE)", grant number 52693-1.

Appendix A. Supplementary data

Supplementary data to this article can be found online at https://doi.org/10.1016/j.enconman.2025.120791.

Data availability

Data will be made available on request.

References

[1] Lowder SK, Skoet J, Raney T. The number, size, and distribution of farms, smallholder farms, and family farms worldwide. World Dev 2016;87:16–29.
[2] Fiorentino G, Zucaro A, Cerbone A, Giocoli A, Motola V, Rinaldi C, et al. The contribution of biogas to the electricity supply chain: an italian life cycle assessment database. Energies 2024;17(13):3264.
[3] EBA Statistical Report 2023. https://www.europeanbiogas.eu/eba-statistical-report-2023/ (Accessed 15 March 2025).
[4] Temiz M, Sinbuathong N, Dincer I. Development and assessment of a new agrivoltaic-biogas energy system for sustainable communities. Int J Energy Res 2022;46(13):18663–75.
[5] Bambokela, J.E., Belaid, M., Muzenda, E. (2020). Preliminary design of a biogas-solar PV hybrid minigrid system for off-grid agricultural communities.
[6] Sieborg MU, Engelbrecht N, Ottosen LDM, Kofoed MVW. Sunshine-to-fuel: demonstration of coupled photovoltaic-driven biomethanation operation, process, and techno-economical evaluation. Energ Conver Manage 2024;299:117767.
[7] Su B, Wang H, Zhang X, He H, Zheng J. Using photovoltaic thermal technology to enhance biomethane generation via biogas upgrading in anaerobic digestion. Energ Conver Manage 2021;235:113965.
[8] Álvaro AG, Palomar CR, Torre RM, Redondo DH, de Godos Crespo I. Hybridization of anaerobic digestion with solar energy: a solution for isolated livestock farms. Energy Convers Manage: X 2023;20:100488.
[9] Hao Y, Li W, Tian Z, Campana PE, Li H, Jin H, et al. Integration of concentrating PVs in anaerobic digestion for biomethane production. Appl Energy 2018;231:80–8.
[10] Calise F, Cappiello FL, Cimmino L, d'Accadia MD, Vicidomini M. Integration of photovoltaic panels and solar collectors into a plant producing biomethane for the transport sector: dynamic simulation and case study. Heliyon 2023;9(4).
[11] Akarsu RT, Demir N. Techno-economic and environmental analysis of biogas-based hybrid renewable energy systems: a case study for a small-scale livestock farm. Process Saf Environ Prot 2024;191:1968–81.
[12] Murano R, Maisano N, Selvaggi R, Pappalardo G, Pecorino B. Critical issues and opportunities for producing biomethane in Italy. Energies 2021;14(9):2431.
[13] Bortoluzzi G, Gatti M, Sogni A, Consonni S. Biomethane production from agricultural resources in the Italian scenario: techno-economic analysis of water wash. Chem Eng Trans 2014;37.
[14] Carfora A, Pansini RV, Romano AA, Scandurra G. Renewable energy development and green public policies complementarities: the case of developed and developing countries. Renew Energy 2018;115:741–9.
[15] Baccioli A, Antonelli M, Frigo S, Desideri U, Pasini G. Small scale bio-LNG plant: comparison of different biogas upgrading techniques. Appl Energy 2018;217:328–35.
[16] Dupraz C. Assessment of the ground coverage ratio of agrivoltaic systems as a proxy for potential crop productivity. Agrofor Syst 2023.
[17] Taramasso MA, Motaghi M, Casasso A. A techno-economic feasibility analysis of solutions to cover the thermal and electrical demands of anaerobic digesters. Renew Energy 2024;121485.
[18] CIB - Consorzio Italiano Biogas. (2024). Biomethane feed-in tariff. https://www.consorziobiogas.it (Accessed 15 March 2025).
[19] Petrollese M, Cocco D. Techno-economic assessment of hybrid CSP-biogas power plants. Renew Energy 2020;155:420–31.
[20] ATTSU Group Company. https://www.attsu.com/en. (Accessed 15 March 2025).
[21] Bina SM, Fujii H, Tsuya S, Kosukegawa H. Comparative study of hybrid ground source heat pump in cooling and heating dominant climates. Energy Conv Manage 2022;252:115122.
[22] Viessmann Company. https://www.viessmann.ch/it/prodotti/pompa-di-calore/vitocal-350-g-pro.html. (Accessed 15 March 2025).
[23] Yang Z, Zhuo Y, Ercang L, Yuan Z. Travelling-wave thermoacoustic high-temperature heat pump for industrial waste heat recovery. Energy 2014;77:397–402.
[24] Van De Bor DM, Infante Ferreira CA. Quick selection of industrial heat pump types including the impact of thermodynamic losses. Energy 2013;53:312–22.
[25] Ennemiri N, Berrada A, Emrani A, Abdelmajid J, El Mrabet R. Optimization of an off-grid PV/biogas/battery hybrid energy system for electrification: a case study in a commercial platform in Morocco. Energy Conv Manage: X 2024;21:100508.
[26] Pöschl M, Ward S, Owende P. Evaluation of energy efficiency of various biogas production and utilization pathways. Appl Energy 2010;87(11):3305–21.
[27] TEDOM Group. https://www.tedom.com/en/. (Accessed 15 March 2025).
[28] Zainali, S., Lu, S. M., Potenza, E., Stridh, B., Avelin, A., & Campana, P. E. (2023). 3D View Factor Power Output Modeling of Bifacial Fixed, Single, and Dual-Axis Agrivoltaic Systems. In AgriVoltaics Conference Proceedings (Vol. 2).
[29] Lu, S. M., Zainali, S., Sundström, E., Nygren, A., Stridh, B., Avelin, A., & Campana, P. (2023). Validation of Vertical Bifacial Agrivoltaic and Other Systems Modeling Effect of Dynamic Albedo on Irradiance and Power Output Estimations. In AgriVoltaics Conference Proceedings (Vol. 2).
[30] Campana PE, Stridh B, Hörndahl T, Svensson SE, Zainali S, Lu SM, et al. Experimental results, integrated model validation, and economic aspects of agrivoltaic systems at northern latitudes. J Clean Prod 2024;437:140235.
[31] Bellone Y, Croci M, Impollonia G, Zad AN, Colauzzi M, Campana PE, et al. Simulation-based decision support for agrivoltaic systems. Appl Energy 2024;369:123490.
[32] Biavetti I, Karetsos S, Ceglar A, Toreti A, Panagos P. European meteorological data: contribution to research, development, and policy support 2014;9229:31–9.

[33] Tong J, Xie L, Fang S, Yang W, Zhang K. Hourly solar irradiance forecasting based on encoder-decoder model using series decomposition and dynamic error compensation. Energy Conv Manage 2022;270:116049.
[34] Ibrahim IA, Khatib T. A novel hybrid model for hourly global solar radiation prediction using random forests technique and firefly algorithm. Energy Conv Manage 2017;138:413–25.
[35] Wang JJ, Jing YY, Zhang CF, Zhao JH. Review on multi-criteria decision analysis aid in sustainable energy decision-making. Renew Sustain Energy Rev 2009;13(9):2263–78.
[36] Kumar A, Sah B, Singh AR, Deng Y, He X, Kumar P, et al. A review of multi criteria decision making (MCDM) towards sustainable renewable energy development. Renew Sustain Energy Rev 2017;69:596–609.
[37] Salmeron JL, Vidal R, Mena A. Ranking fuzzy cognitive map based scenarios with TOPSIS. Expert Syst Appl 2012;39(3):2443–50.
[38] Cabral, J.B., Luczywo, N.A., Zanazzi, J.L. (2016). Scikit-Criteria: Colección de métodos de análisis multi-criterio integrado al stack científico de Python. In XIV Simposio Argentino de Investigación Operativa (SIO 2016)-JAIIO 45 (Tres de Febrero, 2016).
[39] The PVSOL software, Version R8, 2024. Available at: https://pvsol.software/en/ (Accessed: 15 March 2025).
[40] Ebaid MS, Qandil H, Hammad M. A unified approach for designing a photovoltaic solar system for the underground water pumping well-34 at Disi aquifer. Energy Conv Manage 2013;75:780–95.
[41] Urs RR, Sadiq M, Jaradat R, Mayyas A. Harvesting energy horizons: bifacial PV and reversible fuel cells unite for sustainable building solutions. Int J Hydrogen Energy 2024.
[42] Nikzad A, Chahartaghi M, Ahmadi MH. Technical, economic, and environmental modeling of solar water pump for irrigation of rice in Mazandaran province in Iran: a case study. J Clean Prod 2019;239:118007.
[43] Huawei Technologies Co., Ltd., https://solar.huawei.com//media/Solar/attachment/pdf/it/datasheet/LUNA2000-5-15-S0.pdf (Accessed 15 March 2025).
[44] Ravilla A, Shirkey G, Chen J, Jarchow M, Stary O, Celik I. Techno-economic and life cycle assessment of agrivoltaic system (AVS) designs. Sci Total Environ 2024;912:169274.
[45] Messenger RA, Ventre J. Photovoltaic Systems Engineering. CRC Press; 2010.
[46] Ali MS, Ali SU, Mian Qaisar S, Waqar A, Haroon F, Alzahrani A. Techno-economic analysis of hybrid renewable energy-based electricity supply to Gwadar. Pakistan Sustain 2022;14(23):16281.
[47] Calise F, Cappiello FL, Cimmino L, d'Accadia MD, Vicidomini M. Dynamic analysis and thermoeconomic optimization of a Power-to-Gas system driven by renewables. Energy Conv Manage 2024;313:118647.
[48] Di Micco S, Romano F, Jannelli E, Perna A, Minutillo M. Techno-economic analysis of a multi-energy system for the co-production of green hydrogen, renewable electricity, and heat. Int J Hydrogen Energy 2023;48(81):31457–67.
[49] Reher T, Lavaert C, Willockx B, Huyghe Y, Bisschop J, Martens JA, et al. Potential of sugar beet (Beta vulgaris) and wheat (Triticum aestivum) production in vertical bifacial, tracked, or elevated agrivoltaic systems in Belgium. Appl Energy 2024;359:122679.
[50] Agostini A, Colauzzi M, Amaducci S. Innovative agrivoltaic systems to produce sustainable energy: an economic and environmental assessment. Appl Energy 2021;281:116102.
[51] Zidane TEK, Zainali S, Bellone Y, Guezgouz M, Khosravi A, Lu SM, et al. Economic evaluation of one-axis, vertical, and elevated agrivoltaic systems across Europe: a Monte Carlo Analysis. Appl Energy 2025;391:125826.
[52] Zainali, S., Lu, S. M., Bellone, Y., & Campana, P. E. (2025). Optimisation of Agrivoltaic Systems within the Water-Energy-Food Nexus.
[53] Willockx B, Lavaert C, Cappelle J. Performance evaluation of vertical bifacial and single-axis tracked agrivoltaic systems on arable land. Renew Energy 2023;217:119181.
[54] Noussan M, Negro V, Prussi M, Chiaramonti D. The potential role of biomethane for the decarbonization of transport: an analysis of 2030 scenarios in Italy. Appl Energy 2024;355:122322.
[55] Zad AN, Agostini A, Impollonia G, Zainali S, Croci M, Colauzzi M, et al. Life cycle assessment of various agrivoltaic systems across Europe. Sustain Prod Cons 2025;60:260–80.